IJMCM
Autumn 2021, Vol 10, No 4
DOI: 10.22088/IJMCM.BUMS.10.4.265

Original Article

Induction of Apoptosis in the U937 Cell Line Co-cultured with Adipose-derived Stem Cells Secreting Bone Morphogenetic Protein-4

Mostafa Ghorban Khan Tafreshi, Zohreh Mazaheri*, Mansour Heidari, Nahid Babaei, Abbas Doosti

Department of Molecular Cell Biology and Genetics, Bushehr Branch, Islamic Azad University, Bushehr, Iran.

Submmited 29 September 2021; Accepted 17 April 2022; Published 6 June 2022

Transforming growth factor-beta (TGF-β) plays a significant role in tumorigenesis. MiR-181b is a multifunctional miRNA involved in numerous cellular processes, such as cell fate and cell invasion. This study aimed to examine whether the co-culture of adipose-derived stem cells (ADSCs), highly expressing bone morphogenetic protein-4, with the U937 cell line, which is a human myeloid leukemia cell line, is able to induce cell death in this cancer cell line, considering the potential ability of ADSCs to migrate from tumor sites. Cell surface markers, namely CD73 and CD105, were analyzed to verify the identity of mesenchymal stem cells isolated from adipose tissue. Besides, the osteogenic and adipogenic differentiation potentials of ADSCs were evaluated. The induction of cell death and apoptosis in the U937 cell line was assessed using MTT and annexin V/ PI assays, respectively. The expression levels of miR-181 and *TGF-β* were determined in the co-culture system using real-time PCR. The results of MTT and annexin V/ PI assays showed that BMP4-expressing ADSCs could inhibit cell viability and induce apoptosis in U937 cells in the co-culture system. The co-culture of ADSCs, highly expressing BMP-4, with the U937 cell line led to the downregulation of miR-181 and *TGF-β* genes in the human cancer cell line. ADSCs may further be studied as a candidate for the treatment of hematological cancers.

Key words: Stem cells, cancer, *miR-181*, TGF-β, *apoptosis*

The epidemiological studies indicated that obesity and cancer are the leading causes of death in the world (1). Leukemias are caused by abnormal proliferation and differentiation of blood cells and their constituent tissue (bone marrow) and lack of differentiation of hematopoietic cells (2). One of the causes of recurrence and metastasis after treatment is the low number of undifferentiated cells with high reproducibility (3, 4). The type of treatment and the prognosis of cancer vary depending on the stage and advancement of the disease (5, 6). The disease occurs in 35-40% of cases under 60 years and 5-15% in individuals over 60 years (7, 8). Most patients are resistant to

*Corresponding author: Department of Molecular Cell Biology and Genetics, Bushehr Branch, Islamic Azad University, Bushehr, Iran.
Email: z_mazaheri@modares.ac.ir

[DOI: 10.22088/IJMCM.BUMS.10.4.265]

conventional therapies or have a relapse after treatment. The average survival has been reported to be about three months (9). Other treatment approaches include stem cell transplantation, radiotherapy, and the use of chemotherapeutic agents such as daunorubicin (10, 11). New therapies in the research phase include targeted drugs, such as tyrosine kinase signaling inhibitors, as well as gene and cell therapy (12, 13). Another type of treatment that involves the genetic manipulation of cells to induce the secretion of specific protein factors, including the production of a growth factor (e.g., bone morphogenetic protein-4 (BMP4)), could be a new approach in this area. Studies have shown that genetically engineered cells capable of secreting BMP4 play a role in the differentiation of cancer cells into more distinct cell lines that are sensitive to chemotherapy drugs.

U-937 cells are widely used to examine candidate chemotherapeutic compounds in biomedical research. These cells were isolated from the histiocytic lymphoma of a 37-year-old man in 1976 and used to study the differentiation and behavior of monocytes (14). These cells are non-adhesive and grow in suspension, possess a round shape, large rod nucleus, and short microvilli (15). These monocytes can transform into macrophages or dendritic cells. In response to some stimuli, they acquire the morphology and characteristics of macrophages and become the precursors of the mononuclear phagocyte system (16). The differentiation and maturation of monocytes are influenced by a number of microenvironmental conditions. Previous data have shown that U937 cells are affected by several chemicals, such as dimethyl sulfoxide (DMSO), phorbol-12-myristate-13-acetate (PMA), Zn^{2+}, retinoic acid, and 12-O-tetradecanoylphorbol-13-acetate (TPA) (17). U937 cells have some significant biological properties and functions in wound healing and response to biomaterials and pathogens. Thus U937 cells have been widely used to study apoptosis (14,18)

BMP4 belongs to the bone morphogenetic protein family and the beta-growth factor (TGF-β) superfamily transporter (19, 20). The expression of BMP4 is mainly induced by the Smad signaling pathway, and it effectively induces the expression of some microRNAs in the cancer treatment process (21, 22). Langebrake et al. demonstrated the importance of microRNAs (miRNAs) in chronic lymphocytic leukemia for the first time (23). It is now known that the function and activity of miRNAs are altered and lead to the aberrant expression of genes in these types of cells (24). Other genetic mechanisms involved in tumorigenesis include mutations in the Pir-miRNA sequence, changes in single nucleotide polymorphisms (SNP), and abnormal transcription of some oncogene/ tumor suppressor genes (25). Several lines of evidence demonstrate that a number of miRNAs can reflect the progression and differentiation of tumors. In this context, a group of miRNAs is able to act as oncogenes or tumor suppressors (26, 27). It has been shown that the overexpression of miR-181a contributes to the development of acute myeloid leukemia (AML). The inhibition of miR-181a results in the resistance of cancer cells to chemotherapy and natural killer cell (NK-cell) killing (28, 29). This study attempts to induce the differentiation process in the U937 cell line using the secretion of the recombinant BMP4 protein produced by genetically engineered cells (BMP-4- expressing adipose- derived mesenchymal stem cells (ADSCs)) to induce apoptosis in differentiated resistant cells and affect their sensitivity to chemotherapeutic compounds.

Materials and methods

Cell isolation and culture

The obtained samples included male adipose tissues (n= 9 men) with an age range of 25-40 years old who underwent liposuction in Imam Khomeini Hospital. All subjects signed informed consent. The obtained tissues were rinsed several times with

[DOI: 10.22088/IJMCM.BUMS.10.4.265]

phosphate-buffered saline (PBS) supplemented with penicillin and streptomycin (Gibco, Germany). The isolated tissues were then sectioned into small pieces, treated with an equal volume of 0.075% type I collagenase (Sigma, Germany), and subjected to a constant agitation at 37 °C for 1 h. The enzyme inactivation was performed by Dulbecco's Modified Eagle Medium (DMEM) high glucose without glycerophosphate (Sigma, Belgium) supplemented with 10% fetal bovine serum (Gibco, UK), and the resulting mixture was centrifuged at 1200 × g for 10 min to obtain a high-density cell pellet (Clinical Benchtop Centrifuges). The resultant supernatant was discarded and mixed with a stromal vascular fraction (SVF) pellet and 2 ml DMEM medium. The suspended cells were subsequently passed through a 100-µm nylon filter mesh (Falcon Company, USA) and then cultured in DMEM containing 10% fetal bovine serum (FBS) and incubated at 37 °C in a 5% CO_2 incubator. The cell culture medium was replaced with a fresh one every two days.

Characterization of ADSCs by flow cytometry

The isolated ADSCs were washed three times in PBS, centrifuged at 400 × g for 5 min, and then resuspended in ice-cold PBS. Next, the cells were fixed with fresh 4% paraformaldehyde solution (pH 7.2) at room temperature for 5 min. To block non-specific bindings, the cells were rinsed with 10% BSA/PBS for 30 min, washed three times in PBS, and incubated with mouse anti-human CD73 (Abcam, Germany), Rabbit anti-human CD105 (Abcam, Germany), Rabbit anti-human CD34 (Abcam, Germany) and rabbit anti-human CD45 (Abcam, Germany) as primary antibodies at 4°C for 1 h. Then, the samples were rinsed three times with PBS and incubated with rabbit anti-mouse IgG conjugated with FITC as a secondary antibody (at a ratio of 1:100) at 37 °C for 30 min in the dark. Afterwards, the cells were washed twice in PBS, centrifuged at 400 × g for 5 min, and evaluated by a flow cytometry analyzer (Olympus, Japan).

Adipogenic differentiation

The isolated ADSCs at passage 4 were exposed to the adipogenic maintenance medium containing 50 µg/mL indomethacin, 50 µg/mL ascorbic acid, and 100 nM dexamethasone (all chemicals were from Sigma, Germany) for 21 days. The medium was changed every three days, and the adipogenic differentiation was examined using the Oil Red O (Sigma, Germany) staining method. Afterwards, the adipogenic medium was removed, and the cells were washed three times in PBS, then fixed by immersing into 10% formalin for 30-60 min at room temperature. Then, the cells were washed with distilled water and treated with 2 mL isopropanol (60%) for 5 min. Next, isopropanol was removed, and the cells were stained with Oil Red O (2 mL to each well) at room temperature for 5 min. Finally, the cells were rinsed with tap water and visualized under an inverted microscope (Olympus, Japan).

Osteogenic differentiation

The culture medium of ADSCs was changed to the osteogenic maintenance medium containing 10 mM β-glycerophosphate, 0.2 mM ascorbic acid, and 7-10 M dexamethasone (all chemicals were from Sigma, UK), and the cells were maintained in this medium for 21 days. The cell culture medium was replaced with the fresh differentiating medium every three days. To confirm the differentiation of ADSCs into osteogenic cells, Alizarin Red S staining was conducted. In this assay, the osteogenic medium was discarded, and the cells were washed with PBS three times. The cells were then fixed in 70% ethanol at 4 °C for 1 h. Next, cells were rinsed with deionized water and air-dried. The fixed cells were stained with 2% Alizarin Red S (pH 7.2, Sigma, Belgium) at 37 °C for 1 h, washed in deionized water, and examined under an inverted microscope (Olympus, Japan)

Preparation of BMP4- expressing lentiviral vectors

The Lenti-Pac™ HIV Expression Packaging Kit

[DOI: 10.22088/IJMCM.BUMS.10.4.265]

containing a lentiviral vector expressing BMP4 and an empty lentiviral vector as a control vector (abmGood. Co, Canada) was used. All vectors were separately transformed into *E.coli* DH5α to provide high copies of vectors required for cell transfection, and then were extracted and purified from a fresh overnight-grown transformed DH5α bacteria according to available standard protocols. The purified lentiviral vectors were stored at -70 °C until use.

Study design

In this study, three cell groups were utilized to analyze the impact of the co-culture of ADSCs with the U937 cell line on apoptosis induction of cancer cells. These groups included (1) U937 cells, (2) ADSCs+U937 co-culture, and (3) B-ADSCs+U937 co-culture. B-ADSCs imply transfected ADSCs expressing BMP4 with the help of lentiviral vectors. This current research was approved by the Human Ethics Committee of Azad University.

Cell cytotoxicity assay

The cell viability was measured using the MTT (3-(4, 5-Dimethylthiazol-2-yl)-2 and 5-diphenyltetra-zolium bromide, Atocel, Austria) assay to determine the cytotoxicity of BMP4-expressing lentiviral vectors against ADSCs. Briefly, 1×10^4 cells were seeded on 96 well-plates and incubated at 37 °C overnight to allow the cells to adhere. ADSCs were transfected with multiple concentrations of BMP4-expressing lentiviral vectors, including 0, 0.25, 0.5, and 1 µg of the corresponding vector. After the transfection process, ADSCs were incubated with the MTT solution (5 mg/mL) for 4 h at 37 °C. Afterwards, the cell culture medium was removed, and 100 µl dimethyl sulfoxide (DMSO) (Merck, Germany) was added to each well to solubilize formazan crystals. Next, the optical absorbance was measured using an enzyme-linked immunosorbent assay (ELISA) reader (Bio-Rad Laboratories, USA) at 570 nm wavelength. The viability percentage of ADSCs was evaluated by comparing the absorbance of treated cells with control cells.

ADSCs transfection

For ADSCs transfection with lentiviral vectors, 1×10^6 ADSCs were seeded on a 6-well plate containing DMEM medium supplemented with 10% FBS. Then, the cells were incubated in a 5% CO_2 incubator at 37 °C for 24 h. The next day, the cell culture medium of the growing cells was replaced with a prepared DMEM medium supplemented with 2% FBS. The cell transfection was performed with lentiviral vectors using lipofectamine 3000 (Invitrogen, USA). After 24 h, the green fluorescent protein (GFP) activity was monitored in transfected ADSCs using fluorescent microscopy (Labo Med, USA). The GFP activity was considered as an internal control.

Co-culture of U937 cells with ADSCs

The U937 cell line was purchased from the Pasteur Institute of Iran and then cultured in RPMI-1640 medium (Sigma, Belgium) supplemented with 10% FBS (Gibco, UK). To perform the co-culture system, transfected ADSCs expressing BMP4 were seeded at a density of 5×10^4 cells/well onto a 24-well plate and incubated at 37 °C for 24 h. The next day, the U937 cells at a density of 1×10^5 were added to transfected ADSCs and allowed to grow in RPMI-1640 medium supplemented with 10% FBS.

Annexin-V staining

The U937 cell line, ADSCs, and B-ADSCs were collected after co-culturing and washed once with a culture medium supplemented with 2 mm CaCl2 in the absence of phenol red. After discarding the supernatant, 5 µL annexin-V conjugate was added to the residual volume (approximately 130 µL). After incubation for 45 min at room temperature, the cells were washed twice, then suspended in the same medium containing 1 µg/mL phosphatidyl inositol (PI). The samples were analyzed using FACSCalibur (BD Biosciences, San Jose, CA, USA).

RNA isolation and RT-qPCR

The total RNA was extracted from the U937

[DOI: 10.22088/IJMCM.BUMS.10.4.265]

Table1. Sequence of primers.

Genes	Sequences (5´-3´)	Accession NO.
BMP4	F:CGGGACAGGAAGAAGAATAAGAA R:GAATGGTTGGTTGAGTTGAGGTG	NM_001202.6
BMPR1	F: AGATGACCAGGGAGAAACCAC R: CAACATTCTATTGTCCGGCGTA	NM_004329
TGF-β	F: CCCAGCATCTGCAAAGCTC R: GTCAATGTACAGCTGCCGCA	NM_000660.7
GAPDH	F: GCAGGGATGATGTTCTGG R: CTTTGGTATCGTGGAAGGAC	NM_002046.7
miR-181	SL: GTCGTATCCAGTGCAGGGTCCGAGGTATTCGCACTGGATACGAC ACTCAC F: CGGCGGAACATTCAACGCTGTCG R: CCAGTGCAGGGTCCGAGGTA	NR_029626.1
U6	F: CGCTTCGGCAGCACATATAC R: AAATATGGAACGCTTCACGA	NR_004394.1

F: forward primer; R: reverse primer; SL: stem loop primer.

cell line by Qiazol (Qiazol lysis reagent, USA) according to the manufacturer's instructions. Next, the concentration and purity of the extracted RNA were determined using a NanoDrop ND-100 spectrophotometer (Thermo Scientific, Waltham, MA, USA). Afterwards, RNA was converted into cDNA using the Revert aid cDNA synthesis kit (Fermentas, Germany; 25 µl). In this experiment, 500 ng of the newly-synthesized cDNA was used to analyze the relative gene expression. The PCR reactions were conducted in a total volume of 25 µL containing 12.5 µL SYBR Green Premix 2X (Takara, Shiga, Japan) and 10 pM mixed primers. Thermocycling conditions were 95 °C for 10 s, followed by 40 cycles of denaturation at 94 °C for 5 s, and annealing and extension at 60 °C for 34 s. The Primer3 software was employed for designing the specific primers. The specificity of the designed primers was determined by the NCBI BLAST Tool, and the primer sequences are listed in Table 1. The $2^{-\Delta\Delta Ct}$ method was applied to determine the relative expressions for the *BMP4, BMP4 receptor,* and TGF-β genes. The miR-181 was also detected using RT^2 miRNA First Strand Kit (SA Biosciences). The specific primers of miR-181 and U6 cells were purchased from QIAGEN to carry out real-time PCR. The relative expression was determined using the comparative Ct method ($2^{-\Delta\Delta Ct}$). The Ct values of samples were compared with the Ct value of the internal control gene (*GAPDH*). The real-time PCR reactions were performed on the ABI (Applied Biosystems, USA) detection system. All experiments were performed in triplicate.

The specificity of PCR reactions was also examined by electrophoresis and melting curve analysis.

Statistical analysis

All experiments were conducted in triplicate, and the results were represented as the means and standard deviation (mean± SD). The difference between the experimental groups was analyzed using one-way analysis of variance (ANOVA) followed by Tukeys' post hoc test. The level of the statistical significance was set at $P < 0.05$.

Results

ADSC and U937 Cell culture

The morphology of the attached ADSCs is similar to that of bone marrow mesenchymal stem cells with rapid proliferation, as shown in Figure 1. In the early hours, the cells were floating, and the nucleus was visible. After 24 h, the floated

[DOI: 10.22088/IJMCM.BUMS.10.4.265]

cells adhered to the dish to form fibroblast-like colonies. The loaded ADSCs formed a spindle-like shape (fibroblast-like) with several lipid granules within those cells. After the first passage, the cells showed extensive proliferative capacity (Figure 1A). After the fourth passage and 13 days of incubation, the cells were used for the differentiation analysis. In addition, the image on the right represents U937 cells showing a circular shape (Figure 1B).

ADSCs characterization

The surface marker analyses of the isolated adipose-derived cells showed that about 90% of cells were positive for CD105 (90.1 ± 3), while 76% of cells were positive for CD73 (75.8± 3.61), confirming the mesenchymal feature of the isolated cells. A low percent of cells were positive for CD34 (5.98 ± 1.64) and CD45 (7.15 ± 0.26) markers, which are specific for hematopoietic stem cells, indicating the high purity of the isolated and expanded ADSCs as mesenchymal stem cells (Figure 2).

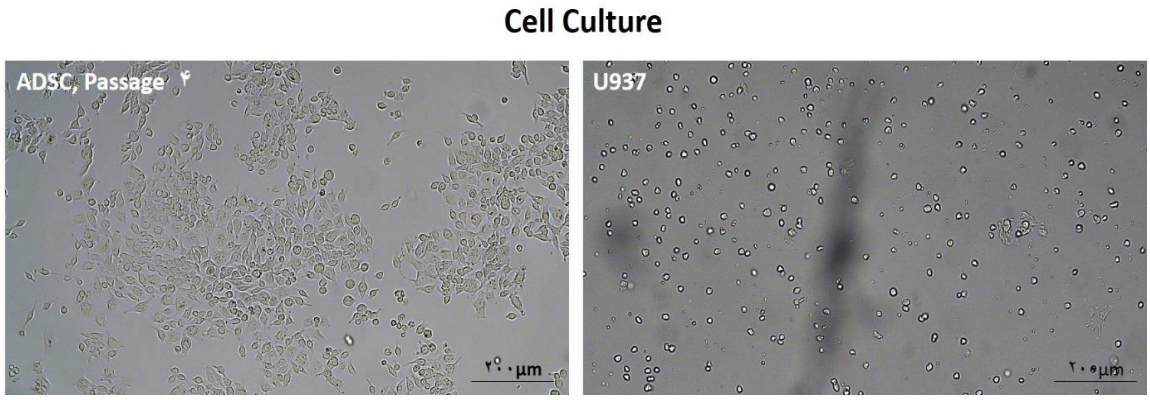

Fig. 1. Morphology of adipose derived stem cells (ADSCs). A: The cells isolated from ADSCs 4th passage, 4 h after incubation; B: U937 cells.

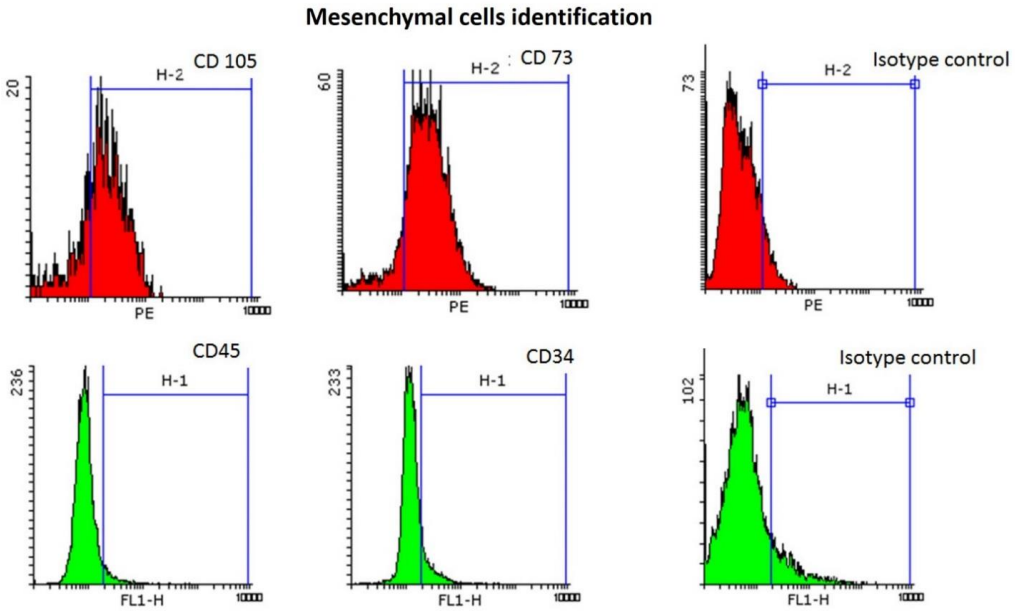

Fig. 2. Surface marker analyses of the isolated adipose-derived cells. From left to right in C part; CD105 = 90.1 ± 3. CD73 = 75.8± 3.61; CD45 = 7.15 ± 0.26; CD34 = 5.98 ± 1.64. The number of positive cells for each marker was assayed by flow cytometry. The data was mean ± SD.

[DOI: 10.22088/IJMCM.BUMS.10.4.265]

The percentage of positive cells was calculated in relation to the negative control,and isotype antibodies were applied for negative control.

Adipogenic and osteogenic differentiation

As shown in Figure 3, ADSCs exhibited a marked differentiation potential into adipogenic and osteogenic lineages. The Oil Red O staining assay showed ADSCs differentiation into the adipogenic lineage, through staining the lipid droplets in differentiated adipocytes (Figure 3A). Furthermore, the Alizarin Red assay confirmed that ADSCs differentiated towards osteoblast under specific differentiation conditions (Figure3B).

BMP4 expression in ADSCs transfected with BMP4-containing lentiviral vector

As shown in Figure 4, ADSCs transfected with BMP4-containing lentiviral vector exhibited a high percentage of GFP-expressing cells, indicating the high efficiency of transfection. Thus, it ensures that GFP-expressing cells also express BMP4 protein in transfected ADSCs.

Cell viability reduction in U937 cells in the co-culture system

The MTT data showed that the cell viability of U937 cells co-cultured with BMP4-expressing ADSCs (B- ADSC +U937 group) for 24 and 72 h significantly decreased in comparison with U937 and ADSC+U937 groups (Figure 5).

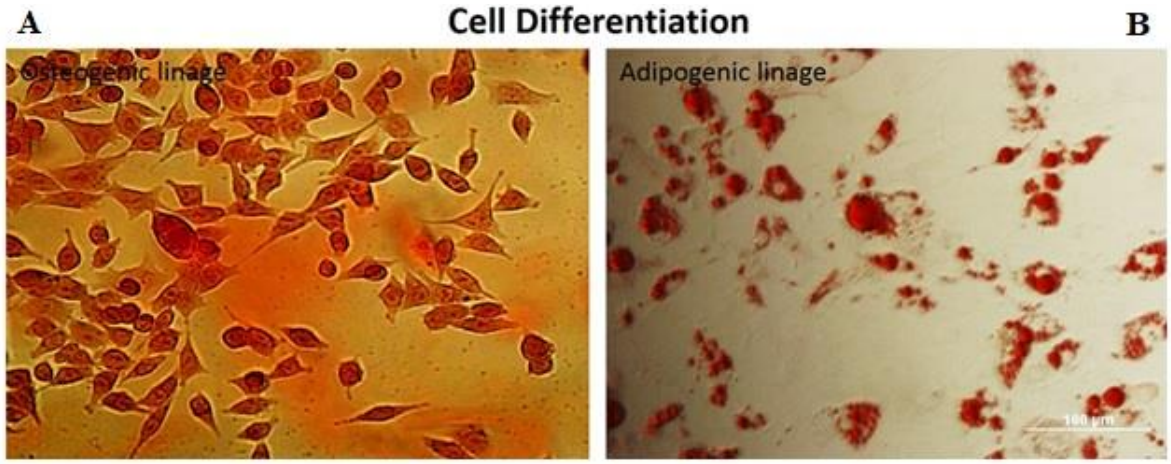

Fig. 3. ***In vitro*** **mesenchymal cells identification.** A: ADSCs after incubation for 21 days in the adipogenic differentiation medium. The cells were visualized with Oil Red O staining; B: ADSCs after incubation for 21 days in the osteogenic differentiation medium. The cells were visualized with Alizarin Red S stain.

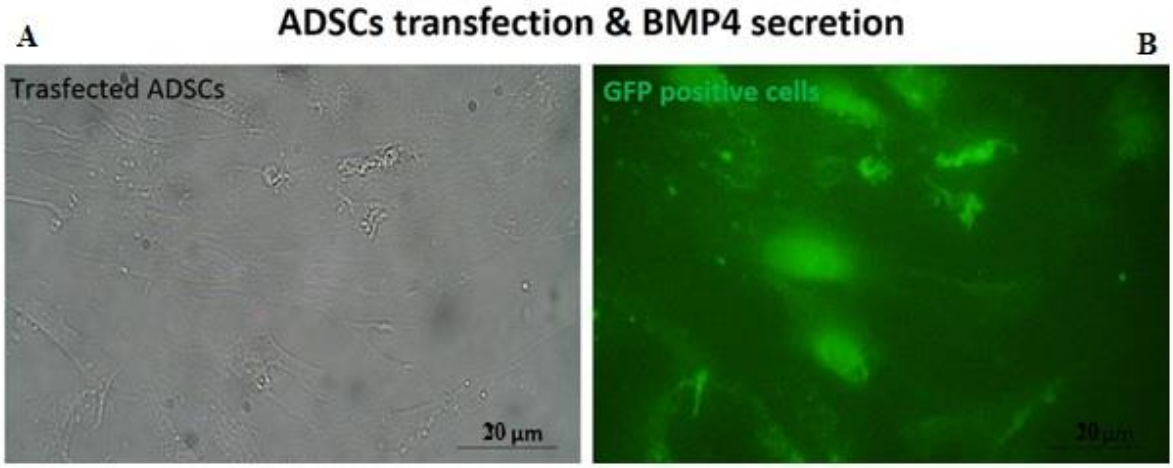

Fig. 4. **DMP4 expression in ADSCs after transfection with lentiviral vector.** GFP-expressing cells were also expressing BMP4 protein in the infected ADSCs.

[DOI: 10.22088/IJMCM.BUMS.10.4.265]

Apoptosis assay

Consistent with the MTT results, the data obtained from the apoptosis assay demonstrated a significant increase in the apoptotic U937 cells in the B-ADSC+U937 group after 72 h in comparison with ADSC-U937 and U937 groups ($P<0.05$) (Figure 6).

Relative gene expression assay

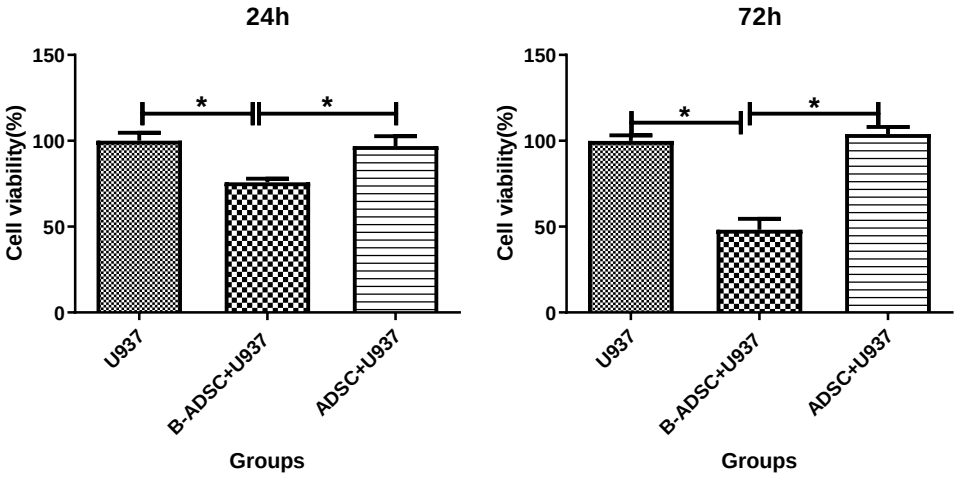

Fig. 5. **Cell viability of U937 cells under co-culture conditions.** Cell viability was assessed after 24 and 72 h. B-ADSC+U937:BMP4-expressing ADSCs co-cultured with U937 cells. (Results are represented as mean ± SD. * shows significant difference ($P \leq 0.01$).

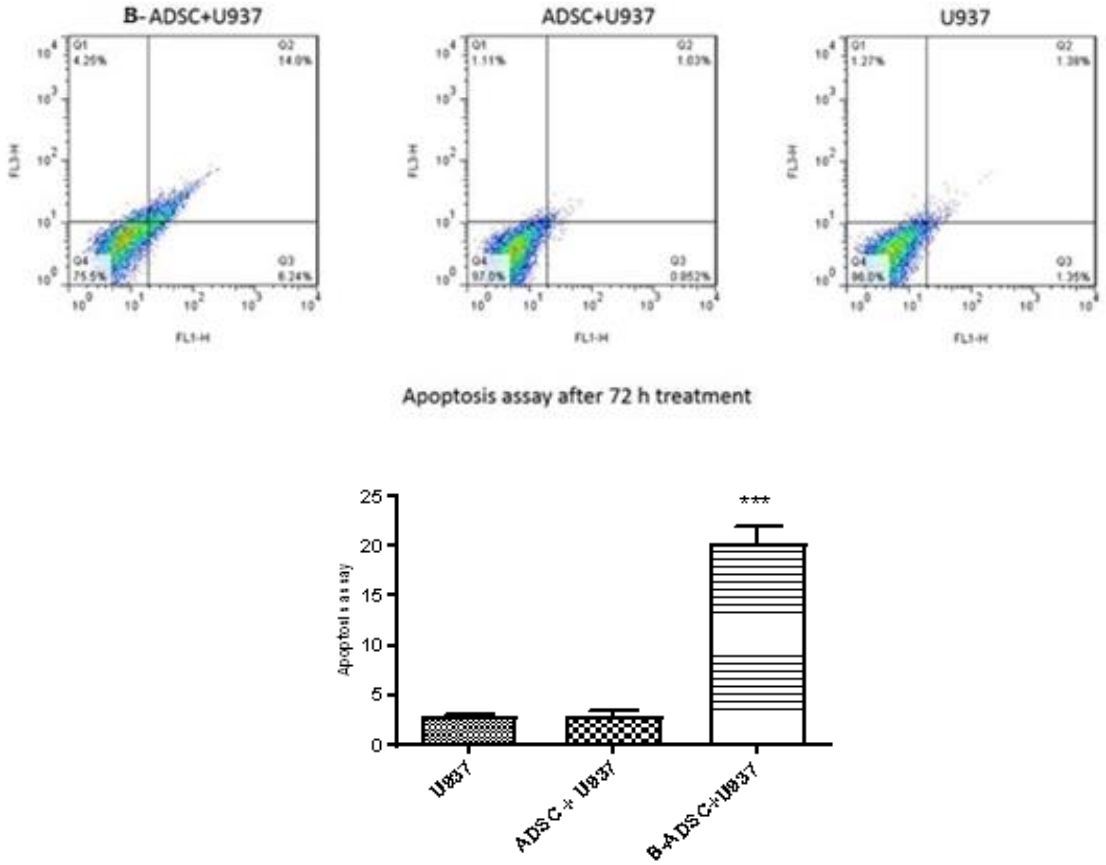

Fig. 6. **Apoptotic assay.** Increase in the apoptotic U937 cells in BMP4-expressing ADSCs co-cultured with U937 cells (B-ADSC+U937) group after 72 h. Results are shown as mean ± SD. *** shows significant difference ($P \leq 0.0001$).

[DOI: 10.22088/IJMCM.BUMS.10.4.265]

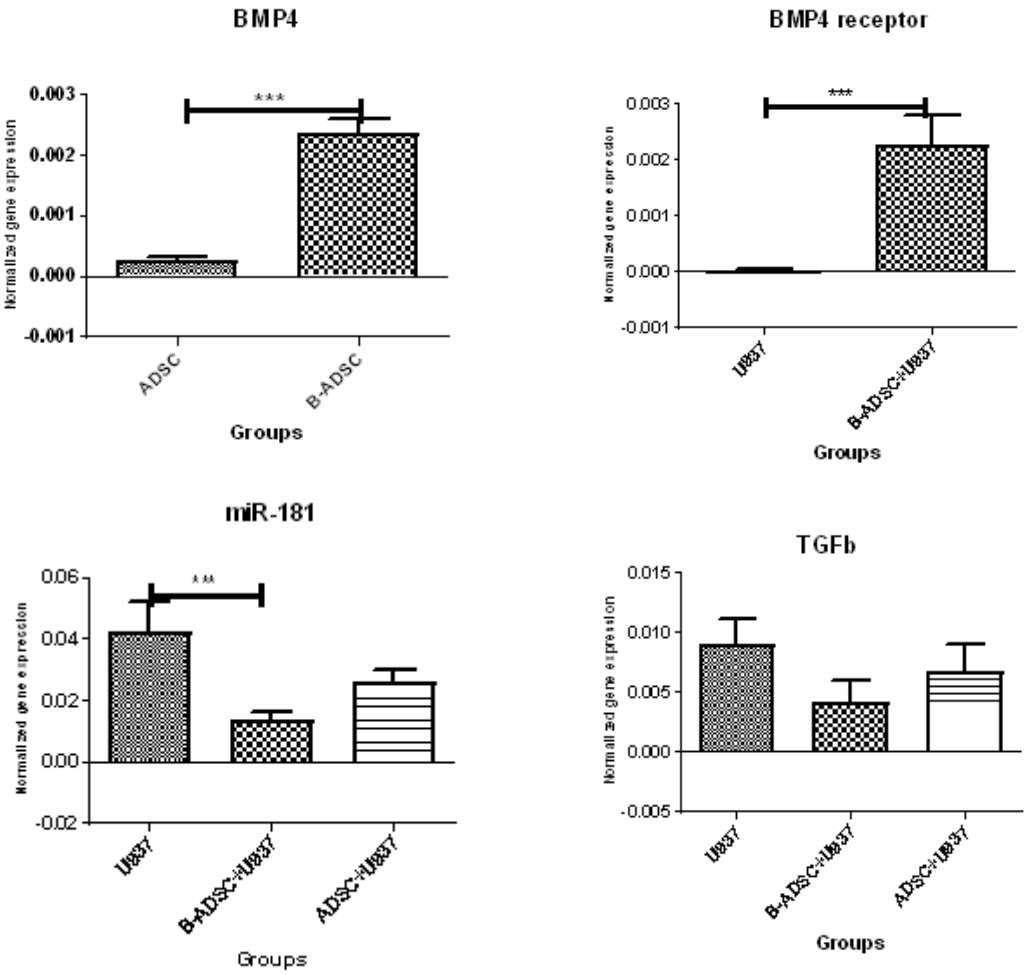

Fig. 7. Expression of *BMP4* and its receptors, miR-181, *TGF-β*. *GAPDH* was applied as internal control. Data was normalized to internal control in each group. Results are shown as mean ± SD. *** shows significant difference ($P \leq 0.0001$).

The results of real-time PCR indicated the overexpression of *BMP4* in ADSCs transfected with BMP4-expressing lentiviral vectors. Besides, upregulation of the BMP4 receptor was detected in U937 cells co-cultured with BMP4-expressing ADSCs (B-ADSCs). Moreover, among the three studied cell groups, the expression levels of miR-181 and *TGF-β* genes were downregulated in the B-ADSC+U937 co-culture group, in comparison with U937 and ADSC+U937 groups. However, the change in the expression of *TGF-β* was not statistically significant (Figure 7).

Discussion

Based on the hypothesis that adipose tissue-derived mesenchymal stem cells can migrate toward the tumoral sites, a cell-based delivery platform was established in which mesenchymal stem cells derived from genetically engineered adipose tissue highly expressed the bone morphogenetic protein (BMP4) as a growth factor belonging to TGF-β family. Our findings showed significant expression of the BMP4 protein in transfected ADSCs secreting BMP4 into the extracellular space. A number of studies showed the antitumor activity of BMP4-TADSCs in U937 cells in which the secreted form of BMP4 is able to induce apoptosis and necrosis in U937 cells under the co-culture conditions. BMP4 is capable of reducing the expression of miR-181 and *TGF-β* genes in U937 cells under the co-culture system. Recently, several lines of evidence have highlighted

[DOI: 10.22088/IJMCM.BUMS.10.4.265]

the role of genetic engineering in establishing new remedial designs in oncology. Choi et al. (2016) published a stem cell-based gene therapy against brainstem glioma by inducing a lentiviral vector expressing tumor necrosis factor-related apoptosis genes in ADSC. They administered the manipulated cells into the brainstems of murine models and found a potent anti-tumor effect (30). Mirzaei et al. described the therapeutic potential of human ADSCs, which were genetically modified to express interferon □-induced protein 10 kDa (IP-10) to inhibit lung metastasis in an immun-ocompetent mouse model of metastatic melanoma (31). In line with these studies, our manipulated ADSCs harboring BMP4 showed therapeutic potential against lymphoma.

BMP4 is a member of the transforming growth factor-β (TGF-β) superfamily and controls cell fate, proliferation, and differentiation. BMP-4 has been shown to exert anticancer activity in breast cancer cells (32). BMP-4 reduces the secretion of granulocyte colony-stimulating factor (G-CSF) and the number and activity of myeloid-derived suppressor cells. A clinical trial study indicated that BMP-4 represses angiogenesis in solid tumors by inducing thrombospondin-1 (*TSP-1*). It has been demonstrated that targeting the BMP-4/SMAD1 signaling would be beneficial to suppress tumor invasion and migration in hepatocellular carcinoma(HCC) (33). Takahashi et al. revealed that the induction of BMP4 led to the suppression of the proliferation of some leukemia/ lymphoma cell lines. They suggested that the regulation of BMP4 signaling may be a valuable therapeutic approach for the treatment of leukemia/lymphoma (34). Our results were in line with previous studies, as BMP4 induced apoptosis and reduced cell survival in the leukemia cell line.

At the gene level, the proliferative inhibitory activity and induction of differentiation of BMP4-ADSCs were associated with inhibition of miR-181 and *TGF-β* expression in U937 cells. Various investigations have shown that specific miRNAs have essential roles in the development of several types of cancer. Zhi et al. and Xiang et al. reported that an increase in miR-181b expression was correlated with a lower prognosis, as shown by the higher overall survival or complete remission in AML patients (35,36). Besides, Butrym et al. indicated that AML patients with lower expression of miR-181a exhibited higher survival rates (37). Numerous studies have demonstrated that specific miRNAs have undeniable roles in various types of cancer. An increase in TGF-β levels can cause myelofibrosis, and its effects on the immune system and stroma may lead to the pathogenesis of some blood malignancies. The regulation of the TGF-β signaling pathway may pave the way for hematologic malignancies therapy. In the present study, a new strategy based on BMP4 induction was designed to significantly repress the cell viability of the leukemia cell line U937. It appears that the use of ADSCs could be useful for the treatment of hematological cancer; however, further studies are warranted to unravel the *in vivo* effect of this type of cell therapy on the amelioration of blood malignancies.

Ethics statement

Acknowledgments

The current study was funded by the Department of Molecular Cell Biology and Genetics, Bushehr Branch, Islamic Azad University, Bushehr, Iran. We thank our colleagues from Histogenotech Company, Tehran, Iran, who greatly assisted us in the implementation of the research.

Conflict of Interest

The authors declare no conflict of interest.

References

1. Bray F, Ferlay J, Soerjomataram I, et al. Global cancer statistics 2018: GLOBOCAN estimates of incidence and mortality worldwide for 36 cancers in 185 countries. CA Cancer

[DOI: 10.22088/IJMCM.BUMS.10.4.265]

J Clin 2018;68:394-424.

2. Ward ZJ, Yeh JM, Bhakta N, et al. Estimating the total incidence of global childhood cancer: a simulation-based analysis. Lancet Oncol 2019;20:483-93.

3. Ogurtsova K, da Rocha Fernandes JD, Huang Y, et al. IDF Diabetes Atlas: Global estimates for the prevalence of diabetes for 2015 and 2040. Diabetes Res Clin Pract 2017;128:40-50.

4. Pulte D, Gondos A, Brenner H. Improvements in survival of adults diagnosed with acute myeloblastic leukemia in the early 21st century. Haematologica 2008;93:594-600.

5. Nachman J, Sather HN, Buckley JD, et al. Young adults 16-21 years of age at diagnosis entered on Childrens Cancer Group acute lymphoblastic leukemia and acute myeloblastic leukemia protocols. Results of treatment. Cancer 1993;71:3377-85.

6. Burnett AK, Hills RK, Milligan D, et al. Identification of patients with acute myeloblastic leukemia who benefit from the addition of gemtuzumab ozogamicin: results of the MRC AML15 trial. J Clin Oncol 2011;29:369-77.

7. Chen YJ, Fang LW, Su WC, et al. Lapatinib induces autophagic cell death and differentiation in acute myeloblastic leukemia. Onco Targets Ther 2016;9:4453-64.

8. Saultz JN, Garzon R. Acute Myeloid Leukemia: A Concise Review. J Clin Med 2016;5.

9. Larson RA. Current use and future development of gemtuzumab ozogamicin. Semin Hematol 2001;38:24-31.

10. Lowenberg B, Ossenkoppele GJ, van Putten W, et al. High-dose daunorubicin in older patients with acute myeloid leukemia. N Engl J Med 2009;361:1235-48.

11. Shu XO, Potter JD, Linet MS, et al. Diagnostic X-rays and ultrasound exposure and risk of childhood acute lymphoblastic leukemia by immunophenotype. Cancer Epidemiol Biomarkers Prev 2002;11:177-85.

12. Abdel-Wahab O, Levine RL. Mutations in epigenetic modifiers in the pathogenesis and therapy of acute myeloid leukemia. Blood 2013;121:3563-72.

13. Binato R, de Almeida Oliveira NC, Du Rocher B, et al. The molecular signature of AML mesenchymal stromal cells reveals candidate genes related to the leukemogenic process. Cancer Lett 2015;369:134-43.

14. Sundstrom C, Nilsson K. Establishment and characterization of a human histiocytic lymphoma cell line (U-937). Int J Cancer 1976;17:565-77.

15. Pagliara P, Lanubile R, Dwikat M, et al. Differentiation of monocytic U937 cells under static magnetic field exposure. Eur J Histochem 2005;49:75-86.

16. Kigerl KA, Gensel JC, Ankeny DP, et al. Identification of two distinct macrophage subsets with divergent effects causing either neurotoxicity or regeneration in the injured mouse spinal cord. J Neurosci 2009;29:13435-44.

17. Prasad A, Sedlarova M, Balukova A, et al. Reactive Oxygen Species Imaging in U937 Cells. Front Physiol 2020;11:552569.

18. Chen X, Zuckerman ST, Kao WJ. Intracellular protein phosphorylation in adherent U937 monocytes mediated by various culture conditions and fibronectin-derived surface ligands. Biomaterials 2005;26:873-82.

19. Fuchs O, Simakova O, Klener P, et al. Inhibition of Smad5 in human hematopoietic progenitors blocks erythroid differentiation induced by BMP4. Blood Cells Mol Dis 2002;28:221-33.

20. Zhao X, Liu J, Peng M, et al. BMP4 is involved in the chemoresistance of myeloid leukemia cells through regulating autophagy-apoptosis balance. Cancer Invest 2013;31:555-62.

21. Azevedo PL, Oliveira NCA, Correa S, et al. Canonical WNT Signaling Pathway is Altered in Mesenchymal Stromal Cells From Acute Myeloid Leukemia Patients And Is Implicated in BMP4 Down-Regulation. Transl Oncol 2019;12:614-25.

22. van den Wijngaard A, Weghuis DO, Boersma CJ, et al. Fine mapping of the human bone morphogenetic protein-4 gene (BMP4) to chromosome 14q22-q23 by in situ hybridization. Genomics 1995;27:559-60.

23. Group M-A-BS, Langebrake C, Creutzig U, et al. Residual disease monitoring in childhood acute myeloid leukemia by multiparameter flow cytometry: the MRD-AML-BFM Study Group. J Clin Oncol 2006;24:3686-92.

24. Corradini E, Babitt JL, Lin HY. The RGM/DRAGON family of BMP co-receptors. Cytokine Growth Factor Rev 2009;20:389-98.

25. Chen H, Liu T, Liu J, et al. Circ-ANAPC7 is Upregulated in Acute Myeloid Leukemia and Appears to Target the MiR-181 Family. Cell Physiol Biochem 2018;47:1998-2007.

26. Wang J, Wang S, Zhou J, et al. miR-424-5p regulates cell proliferation, migration and invasion by targeting doublecortin-like kinase 1 in basal-like breast cancer. Biomed Pharmacother 2018;102:147-52.

[DOI: 10.22088/IJMCM.BUMS.10.4.265]

27. Salem AH, Dunbar M, Agarwal SK. Pharmacokinetics of venetoclax in patients with 17p deletion chronic lymphocytic leukemia. Anticancer Drugs 2017;28:911-4.

28. Negrini M, Nicoloso MS, Calin GA. MicroRNAs and cancer--new paradigms in molecular oncology. Curr Opin Cell Biol 2009;21:470-9.

29. Calin GA, Croce CM. MicroRNA signatures in human cancers. Nat Rev Cancer 2006;6:857-66.

30. Choi SA, Yun JW, Joo KM, et al. Preclinical Biosafety Evaluation of Genetically Modified Human Adipose Tissue-Derived Mesenchymal Stem Cells for Clinical Applications to Brainstem Glioma. Stem Cells Dev 2016;25:897-908.

31. Mirzaei H, Salehi H, Oskuee RK, et al. The therapeutic potential of human adipose-derived mesenchymal stem cells producing CXCL10 in a mouse melanoma lung metastasis model. Cancer Lett 2018;419:30-9.

32. Ren W, Liu Y, Wan S, et al. BMP9 inhibits proliferation and metastasis of HER2-positive SK-BR-3 breast cancer cells through ERK1/2 and PI3K/AKT pathways. PLoS One 2014;9:e96816.

33. Wang Y, Sun B, Zhao X, et al. Twist1-related miR-26b-5p suppresses epithelial-mesenchymal transition, migration and invasion by targeting SMAD1 in hepatocellular carcinoma. Oncotarget 2016;7:24383-401.

34. Takahashi Y, Ishigaki T, Okuhashi Y, et al. Effect of BMP4 on the growth and clonogenicity of human leukemia and lymphoma cells. Anticancer Res 2012;32:2813-7.

35. Zhi F, Cao X, Xie X, et al. Identification of circulating microRNAs as potential biomarkers for detecting acute myeloid leukemia. PLoS One 2013;8:e56718.

36. Xiang L, Li M, Liu Y, et al. The clinical characteristics and prognostic significance of MN1 gene and MN1-associated microRNA expression in adult patients with de novo acute myeloid leukemia. Ann Hematol 2013;92:1063-9.

37. Butrym A, Rybka J, Baczynska D, et al. Expression of microRNA-181 determines response to treatment with azacitidine and predicts survival in elderly patients with acute myeloid leukaemia. Oncol Lett 2016;12:2296-300.

[DOI: 10.22088/IJMCM.BUMS.10.4.265]